Anti-Gr-1 Antibody Provides Short-term Depletion of MDSC in Lymphodepleted Mice With Active-specific Melanoma Therapy

Peter Rose (Peter_Rose@outlook.de)
Department of Cardiac Surgery, University Hospital Heidelberg https://orcid.org/0000-0002-4530-9584
Natasja K. van den Engel
University Hospital Munich Campus Grosshadern: Klinikum der Universitat Munchen Standort Grosshadern
Julia R. Kovacs
University Hospital Munich Campus Grosshadern: Klinikum der Universitat Munchen Standort Grosshadern
Rudolf A. Hatz
University Hospital Munich Campus Grosshadern: Klinikum der Universitat Munchen Standort Grosshadern
Louis Boon
Bioceros
Hauke Winter
Thoraxklinik Heidelberg

Research Article

Keywords: Immunotherapy, Vaccination, Myeloid-Derived Suppressor Cells, Melanoma, T-Lymphocytes

Posted Date: July 9th, 2021

DOI: https://doi.org/10.21203/rs.3.rs-678380/v1

Abstract

Background

Lymphodepletion, reconstitution and active-specific tumor cell vaccination (LRAST) enhances the induction of tumor-specific T cells in a murine melanoma model. Myeloid-derived suppressor cells (MDSC, Gr-1$^+$ CD11b$^+$) may counteract the induction of tumor-reactive T cells and their therapeutic efficacy. Thus, the aim of the study was to evaluate a possible benefit of MDSC depletion using anti-Gr-1 antibodies (Ab) in combination with LRAST.

Methods

Female C57BL/6 mice with 3 days established subcutaneous (s.c.) D5 melanoma were lymphodepleted with cyclophosphamide and reconstituted with naive splenocytes. Vaccination was performed with irradiated syngeneic mGM-CSF-secreting D5G6 melanoma cells. For MDSC depletion, anti-Gr-1 Ab (clone RB6-8C5, 230 µg) was injected every other day starting on the day of lymphodepletion. Induction of tumor-specific T cells derived from tumor vaccine draining lymph nodes (TVDLN) was evaluated by the amount of tumor-specific interferon (IFN)- γ release. Tumor growth was monitored following active-specific vaccination with or without anti-Gr-1 Ab administration.

Results

LRAST combined with anti-Gr-1 mAb administration enhanced the induction of tumor-specific T cells in TVDLN capable of releasing IFN-γ in a tumor-specific manner. In mice treated with LRAST and anti-Gr-1 mAb growth of D5 melanoma cells was significantly delayed for two weeks following tumor injection as compared to mice with LRAST treatment alone. Furthermore, we elucidate the impact of anti-Gr-1 depleting antibodies on the memory T cell compartment.

Conclusion

Our data indicate that standard of care treatment regimens against cancer can be improved by implementing agents, e.g. depleting antibodies, which target and eliminate MDSC.

Background

Immunotherapy has long found its way into melanoma treatment. Recently, immune checkpoint-inhibition of CTLA-4 and PD-1 has emerged as the frontline option for the treatment of patients with advanced stages of the disease, targeting negative regulations of immune responses and thereby activating tumor specific cytotoxic T cells (1–3). In contrast, active-specific immunotherapy engages autologous tumor cells as a whole cell vaccine to provide a variety of potential tumor antigens (4). In many tumors these tumor antigens have not been identified and often represent weak self-antigens, unlikely to induce a robust anti-tumor T cell immune response (5).

Conducting active-specific tumor vaccination in lymphopenic hosts has provided promising results in murine gastric and melanoma models, as well as in mice challenged with cells derived from spontaneously occurring mammary tumors of *neu* transgenic mice (5–7).

This effect might partially result from a lymphopenia-induced proliferative stimulus on pre-existing and newly established tumor-directed T cells, especially when homeostatic proliferation goes in hand with antigen encounter (7–10). Preclinical studies with active-specific and adoptive immunotherapy in a murine melanoma tumor model demonstrated that this strategy enhances the induction of tumor-specific T cells improving therapeutic efficacy (5, 11). Although van den Engel *et al.* and others could show an enhanced anti-tumor immune response using a whole cell vaccine combined with GM-CSF exposure following lymphodepletion (5–7), generating tumor-directed T cells does not necessarily translate into an effective trafficking to the tumor site and tumor cell-killing (12). A major obstacle is a locally immunosuppressive tumor-environment of which MDSC represent a major component (13).

MDSC represent a heterogeneous population of immature myeloid cells and are known for their immunosuppressive properties in the tumor microenvironment (14). Their contribution to an impaired efficacy of immunotherapy has been shown for adoptive cell therapy, dendritic cell (DC) vaccination and checkpoint-inhibition (15). MDSC expansion occurs in pathological conditions, including malignant disease, upon alteration in myelopoiesis followed by accumulation in peripheral lymphoid organs as well as in the tumor microenvironment (13). In mice, MDSC are commonly defined by the co-expression of the myeloid delineation markers CD11b and Gr-1. Based on the expression of the cell surface markers Ly6G and Ly6C the two major subtypes of MDSC with distinct phenotype, morphology, and immunosuppressive properties can be distinguished; $CD11b^{+}$ $Ly6G^{-}$ $Ly6C^{high}$ monocytic (M-MDSC) and $CD11b^{+}$ $Ly6G^{+}$ $Ly6C^{+}$ polymorphonuclear (PMN-) MDSC (13, 16). In the periphery, PMN-MDSC represent the largest portion of MDSC, when up-regulated under different pathological conditions (13, 17). In the tumor environment, MDSC become more suppressive and M-MDSC are outweighing PMN-MDSC in frequency (13, 17, 18). The immunosuppressive capacities of MDSC are mediated in an antigen-specific and non-specific manner (14). In lymphoid organs of the periphery MDSC mainly act antigen-specifically with mechanisms including NO and ROS, nutritional deprivation of T cells from L-arginine, L-tryptophan and L-cysteine, impairment of T cell homing and production of TGF-β and IL-10, thus creating an immunosuppressive milieu. Within the tumor environment MDSC act in a more non-specific way, including up regulation of ARG-1 and iNOS and the inhibitory surface-expression of PD-L1 (13). Regulatory T cells (Treg), a sub-population of $CD4^{+}$ T cells capable of down-regulating anti-tumor immune responses, are induced by MDSC in the periphery and attracted to the tumor site by secretion of the chemokines CCL4 and CCL5 (13, 19).

Different efforts have been made to modulate or even ablate MDSC aiming at improving the outcome of malignant disease in mice and men. There is evidence that depletion of MDSC, e.g. by applying triperpenoids, all-trans-retinoic acids or nitroaspirin, may improve therapeutic efficacy (20). Antibody mediated MDSC-depletion using anti-Gr-1 or anti-Ly6G monoclonal antibodies (mAb) led to a complete but temporary, organ-dependent depletion of MDSC (21–24). Long-term treatment of mice with an anti-

GR1 antibody combined with a therapeutic BMA-OVA vaccination induced a pronounced tumor reduction or even a complete tumor eradication in a murine lung tumor model, as reported by Srivastava *et al* (23).

Thus, a promising approach to improve the therapeutic efficacy of anti-tumor vaccination is the combination of different immunotherapeutic strategies to avoid the threatening possibility of tumor immune escape.

Different leukocyte populations are involved in anti-tumor reactions. Especially high frequencies of $CD8^+$ cytotoxic and memory T cells were found to be associated with better outcomes in most human cancers (25–27). Effector $CD8^+$ T cells (T_{eff}) arise from naive T cells upon antigen-presentation and co-stimulation by antigen-presenting cells. This fundamental process in anti-tumor immunity mainly occurs in TVDLN, but may also happen in direct contact to the tumor. T_{eff} yield robust anti-tumor responses, but lack in durability and long-term activity (28). This in turn is the main characteristic of memory $CD8^+$ T cells, which remain present following first line responses (28, 29). Furthermore, memory $CD8^+$ T cells, in contrast to their effector counterparts, seem to be superior in their cytotoxic abilities (30–32). Both central-memory (T_{cm}) and effector-memory (T_{em}) T cells contribute to an anti-tumor response, where T_{em} rapidly acquire effector function, present with enhanced killing capacity and largely contribute to tumor-specific IFN-γ production (28); T_{cm} in contrast reside in secondary lymphatic tissues due to their expression of CD62L and CCR7 and are characterized by a less pronounced effector status and a more stem-cell-phenotype with strong proliferative capacities, giving rise to T_{em} (and T_{eff}) upon antigen re-stimulation (33, 34). Overall, compared to $T_{em,}$ T_{cm} were shown to have a more prominent role in anti-tumor responses (29, 33, 35).

Here we investigated the therapeutic efficacy of a treatment that combines active-specific tumor-cell vaccination with mGM-CSF-secreting D5 melanoma cells and an antibody-mediated depletion of MDSC in a model of murine D5-melanoma. The aim of the study was to evaluate the frequencies of MDSC and $CD8^+$ T cells following LRAST treatment and to elucidate whether depletion of MDSC would provide a benefit in anti-tumor treatment.

Materials And Methods

Mouse strains and cell lines

Wildtype C57BL/6 mice (WT, Ptprcb = $CD45.2^+$, Charles River Laboratories International, Inc., Sulzfeld, Germany) between 8-12 weeks of age were used for *in vivo* experiments, as well as for the generation of single cell suspensions from lymphatic nodules (LN) and spleen. Congenic B6.SJL-Ptprca Pepcb/BoyCrl mice ($CD45.1^+$; Charles River Laboratories International, Inc., Calco, Italy) served as spleen cell donors for reconstitution of wildtype mice after lymphodepletion. Mice were kept under standard pathogen-free conditions in the animal facility of the Walter-Brendel Center, Ludwig-Maximilian-University, Munich. The animal experiments were performed after approval by the local regulatory agency (Regierung von

Oberbayern, Munich, Germany). B16BL6-D5 (D5) is a poorly immunogenic subclone of B16BL6 melanoma (36). D5-G6 is a clone of D5 that was stable transduced with a murine GM-CSF retroviral MFG vector (provided by Dr. M. Arca, University of Michigan, Ann Arbor, MI). D5-G6 cells secrete approximately 200 ng/ml/10^6 cells / 24 hours GM-CSF.(37) The MCA 310 fibrosarcoma and LLC1 lung carcinoma cell lines were kindly provided by Dr. B.A. Fox (Portland, OR). The gastric cancer cell line mGC8 was established previously from gastric tumors which developed spontaneously in CEA424-SV40 Tag transgenic mice (C57BL/6-Tg(CEACAM5-Tag) L5496Wzm) (38).

Media and reagents

For cell culture of mGC8- and MCA310-cells RPMI 1640 medium was used supplemented with 10 % fetal calf serum (FCS “Gold"; PAA Laboratories, Coelbe), 2 % sodium pyruvate (Invitrogen, Karlsruhe, Germany), 2 % non-essential amino acids (NEAA), 2 % L-glutamine and 0,1 % β-Mercaptoethanol. D5-, D5G6- and LLC1-cells required DMEM medium, containing 10 % FBS, 1 % sodium pyruvate, 1 % NEAA and 2 % L-glutamine.

Preparation of single cell suspensions

Mice were killed by cervical dislocation after inhalation anesthesia with isoflurane (Forene 100 % V/V, Abbott GmbH & Co.KG, Wiesbaden, Germany). Spleen, axillary and inguinal LN (in the following called tumor vaccine – draining LN “TVDLN”, in the case when vaccination has been performed) and tumors were removed under sterile conditions. Organs were disrupted using cannulas and syringe-stomps. Single cells were resuspended with FBS (1 %) containing PBS and filtered over a 100 µm cell-filter.

In vivo treatment of mice (LRAST)

For the *in vivo* experiments lymphodepletion was induced by intraperitoneal (i.p.) injection of 200 mg/kg cyclophosphamide 3 days after tumor inoculation, followed by i.v. reconstitution with 20 x 10^6 naïve CD45.1$^+$ spleen cells and active-specific tumor cell vaccination using 5 – 10 x 10^6 irradiated mGM - CSF-secreting D5G6 - cells. The cyclophosphamide dose was chosen since earlier studies had shown an increased proliferation and long-term survival of antigen-specific T cells at this particular dose, alone or in combination with fludarabine. [18,27] Naïve, non-lymphopenic mice served as control. Tumor development was followed by serial measurements of the tumor diameters and was depicted as tumor size (mm^2) = d × D, where d and D were the shortest and the longest tumor diameter, respectively.

Depletion of MDSC

Starting on the day of lymphodepletion (day 0) 230 µg anti-Gr-1 monoclonal antibodies (clone RB6-8C5) were i.p. injected every other day until mice were euthanized. Anti-phytochromatin antibodies (isotype control) served as control.

In vitro T cell activation and expansion

For T cell analyses mice were vaccinated by s.c. injection with 2,0 × 10^7 irradiated D5G6 tumor cells on four sites near the extremities (5,0 × 10^6 per injection). Where indicated, lymphodepletion and reconstitution were performed as described above. TVDLNs were harvested nine days after vaccination and lymph node cells were polyclonally activated with an anti-CD3 monoclonal antibody (mAb; 5 µg/ml, 2C11, kindly provided by Dr. H.M. Hu, Portland, OR) for 2 days at 4,0 × 10^6 cells/ml in complete medium (CM) in 24 - well plates. Subsequently cells were supplemented with 60 IU / ml of interleukin-2 (IL-2, Proleukin, Chiron, Ratingen, Germany) for 4 days. After 4 days, cytokine release assays were performed as described elsewhere with the following modifications (39): TVDLN cells (10^6 cells) were washed and cultured alone or stimulated with tumor cells (0.2 × 10^6 cells), or immobilized anti-CD3 antibody in 1 ml of CM supplemented with gentamycin (Lonza, Cologne, Germany) and 60 IU IL-2/ml in a 48-well tissue culture plate at 37°C, 5 % CO_2 for 18 h. The tumor targets included the tumor cell line used for vaccination (D5). LLC1, mGC8 and MCA310 tumor cells served as negative controls. Supernatants were analyzed by ELISA.

ELISA

IFN-γ was measured in supernatants by conventional sandwich ELISA, using mAb AN-18 and biotinylated mAb R4-6A2 (BD Biosciences, Heidelberg, Germany). Supernatants were analyzed in duplicate. Extinction was analyzed at 405 / 490 nm on a Spectra Fluor microplate ELISA reader (TECAN, Crailsheim, Germany) with the EasyWin software (TECAN). The detection limit of the ELISA for IFN-γ was 125 pg/ml.

Flow cytometry

For surface staining, cells were washed with PBS and suspended in PBS supplemented with 0.5% (w/v) bovine serum albumin (BSA) and 0.02% (w/v) sodium azide. Non-specific binding of antibodies to Fc receptors was blocked by preincubation of the cells with rat anti-mouse CD16/CD32 monoclonal antibodies 2.4G2 (1 µg/10^6 cells, BD Biosciences) for 15 min. Subsequently, the cells were incubated with the mAb of interest for 30 min at 4°C, washed and analyzed using a FACS Calibur or a LSRII (BD Biosciences). Dead cells were excluded using Zombie Yellow staining. Data were analyzed using the FACS-Diva software (Version 4.0.2) and FlowJo® software (Version 10.5.0). The following reagents and mAbs against murine antigens were used: allophycocyanin (APC)-conjugated anti-mouse/human CD44 (eBioscience), anti-mouse CD8a (Biolegend, including all following), Ly6C; allophycocyanin/Cy7 (APC/Cy7)-conjugated anti-mouse CD3e, Ly6G; fluorescein isothiocyanate (FITC)-conjugated anti-mouse CD45.2; Pacific Blue-conjugated anti-mouse MHC-II; phycoerythrin (PE)-conjugated anti-mouse CD11b, CD3e, CD62L, Ly6G, goat anti-rat IgG; phycoerythrin/Cy7 (PE/Cy7)-conjugated CD8a, CD11b; Peridinin-chlorophyll proteins/Cy5.5 (PerCP/Cy5.5)-conjugated anti-mouse CD45.1.

Statistical analysis

Statistical analysis was performed using GraphPad Prism 7/8 (GraphPad Software Inc., La Jolla, CA 92037 USA). 2-way ANOVA or unpaired Student t test was used as indicated. Values of $p < 0.05$ were

considered to be statistically significant (*p < 0.05; **p < 0.01; ***p < 0.001; ns p > 0.05).

Results

MDSC subsets temporarily accumulate in spleen and peripheral blood after LRAST

The frequencies of $CD11b^+$ $Ly6G^+$ $Ly6C^+$ PMN-MDSC and $CD11b^+$ $Ly6G^-$ $Ly6C^{high}$ M-MDSC were assessed in the peripheral blood and the spleen of tumor-bearing wild type C57BL/6 mice, at indicated time points following lymphodepletion (day 0) and active-specific tumor-cell vaccination (day 1). FACS-analyses were performed starting on the day of lymphodepletion (peripheral blood) or 3 days later (spleen; Fig. 1).

About 7 and 10 days after treatment initiation (LRAST) $CD11b^+$ $MHCII^-$ myeloid cells originating in the recipient mouse ($CD45.2^+$) were significantly increased in the spleen and the peripheral blood (Fig. 1 A and C). We observed a significant increase of $CD45.2^+$ PMN-MDSC in the blood (Fig. 1 C), a remarkable but not significant increase for cells resembling PMN-MDSC in the spleen (Fig. 1 A), and M-MDSC in blood and spleen (Fig. 1 A and C). $CD45.2^+$ PMN-MDSC accounted for 51 % of total $CD45.2^+$ leukocytes in the peripheral blood of tumor-bearing mice, 7 days after LRAST. In contrast, reconstituted $CD45.1^+$ PMN- or M-MDSC from donor mice were not found in a considerable extent in both organs and did not show similar kinetics compared to their $CD45.2^+$ counterparts over time (Fig. 1 B and D). One month following LRAST, frequencies of $CD45.2^+$ PMN- and M-MDSC were back to values comparable to baseline at day 0.

Thus, we hypothesized that the pronounced occurrence of potentially immunosuppressive MDSC following LRAST treatment might be a key limiting factor for treatment efficacy.

RB6-8C5 eliminates MDSC in the initial treatment-phase

As we had hypothesized that MDSC inhibit the induction of tumor specific T cells we injected MDSC depleting antibodies i.p. in combination with LRAST treatment. Dose and dosing interval were chosen according to previous reports regarding antibody-mediated depletion of MDSC for therapeutic and non-therapeutic purposes and in combination with other immunotherapeutic approaches (21-23, 40-43). To deplete MDSC we injected 230 µg anti-Gr-1 mAb i.p. every other day, starting on the day of cyclophosphamide administration (Fig. 2, A). As a control, mice received an equivalent dose of isotype control following the same time schedule. Efficacy of MDSC depletion using anti-Gr-1 Ab was monitored in peripheral blood in short time intervals 24 or 48 hours after the last antibody administration and up to 24 days after treatment initiation (Fig. 3, C).

Due to an identical binding site, staining of Ly6G epitopes with anti-Ly6G (1A8) or anti-Gr-1 fluorochrome-conjugated antibodies is restricted when Gr-1 antibodies (RB6-8C5) are being used. Therefore, to reveal hidden PMN-MDSC and to elucidate the proportion of PMN- and M-MDSC with cell bound RB6-8C5, we used a secondary antibody (“2nd Ab”) approach. Peripheral leukocytes from RB6-8C5-treated mice were

obtained and stained with PE-conjugated goat anti-rat IgG. Corresponding plots (Fig. 2, "2nd Ab+", B) indicate the portion of PMN- and M-MDSC with cell bound RB6-8C5. 48 hours (day 2) and 96 hours (day 4) following first anti-Gr-1 mAb administration a significant depletion of PMN-MDSC was observed (Fig. 2, B / C). Secondary antibody staining revealed no relevant amount of cell-bound RB6-8C5 in the PMN-gate, as well as the neighboring areas (data not shown), on both days. M-MDSC frequencies in mice following MDSC-depletion appeared to be lower, compared to values in mice without RB6-8C5, but failed to significantly reduce MDSC. A portion of the cells located in the M-MDSC gate was bound by RB6-8C5 on day 2 and day 4 (0,6 % on day 2; 1,6 % on day 4).

Thus, anti-Gr-1 mAbs are capable of sufficiently depleting circulating PMN-MDSC while M-MDSC appear to be altered in frequencies, but not depleted.

PMN-MDSC recur despite long-term treatment with RB6-8C5

In our experiments the MDSC depleting antibody was administered i.p. every other day for approximately 4 weeks. Since both MDSC subsets express Ly6C at the surface and anti-Ly6C fluorochrome-conjugated antibodies do not interfere with Rb6-8C5, we plotted $CD11b^+$ $Ly6C^+$ cells to depict all MDSC which exhibit secondary antibody binding over time (Fig. 3, A.), representing the percentage of anti-Gr-1 mAb bound MDSC. Compared to the control, which showed absence of RB6-8C5-binding, the $CD11b^+$ $Ly6C^+$ cells, which represent both MDSC subsets, exhibited increasing RB6-8C5-binding over time, with 0,0% on day 0 (before RB6-8C5 administration), 8,9 % on day 2, 62,8 % on day 4, and 64,6 % on day 7 after the first dose of anti-Gr-1 mAb.

RB6-8C5-bound $CD11b^+$ $MHCII^-$ myeloid cells revealed a dynamic shift within the Ly6G/Ly6C-plot (Fig. 3, B). Red dots, indicating RB6-8C5-bound cells, appear in the Ly6G positive and negative region of the Ly6G / Ly6C-plot, but exhibit equal Ly6C-fluorescence intensity, when comparing different mice of the same treatment group at day 7 (Fig. 3, B). As the significance of antibody-bound MDSC occurring in respective MDSC-gates is not yet clear, we compared adjusted frequencies of PMN- and M-MDSC (all MDSC in the PMN- and M-MDSC gate minus RB6-8C5 -bound cells), as well as overall cell frequencies of respective gates (PMN- and M-MDSC including RB6-8C5-bound cells) from LRAST + RB6-8C5 treated mice to MDSC from mice treated only with LRAST (Fig 3, C and D). In this manner we tried to address whether RB6-8C5 can induce a long-term MDSC-depletion.

Depleting antibody was evident on the surfaces of PMN- and M-MDSC up to day 15 after onset of i.p. antibody administration. The portion of PMN-MDSC net of RB6-8C5-bound cells was significantly reduced on days 7 and 15. Remarkably, when maximum increase of PMN-MDSC after LRAST could be expected (day 7, Fig. 1, C), PMN-MDSC, even including the RB6-8C5-bound portion, were significantly reduced. Nevertheless, on both days (7 and 15) a considerable percentage of PMN-MDSC (less pronounced for M-MDSC) showed RB6-8C5-binding, as indicated by secondary antibody staining. Interestingly, trends for frequency kinetics for M-MDSC appeared to be different from those of PMN-MDSC, with an initial increase seen on day 7, followed by a reduction by day 15. At the end of the

experiment (day 24) both PMN- and M-MDSC frequencies where back to baseline in mice treated with LRAST + RB6-8C5 as compared to the control-group.

These data demonstrate that a successful depletion of MDSC, especially PMN-MDSC, can be achieved for a short period of time, despite continuous administration of depleting antibodies. Further, these long-term results indicate a different impact of anti-Gr-1 mAbs on M-MDSC compared to PMN-MDSC, since no significant depleting effect on M-MDSC and little binding of RB6-8C5 could be observed within 24 days.

MDSC depletion improves vaccination responses

In order to evaluate the effect of MDSC-depletion on the induction of tumor-specific T cells, IFN-g release from TVDLN of LRAST treated mice was assessed. Therefore, TVDLN were isolated nine days following LRAST and analyzed in a cytokine release assay. Cytokine responses were evaluated upon restimulation with D5-melanoma cells or control tumor-cell lines (LLC1, mGC8, MCA310). Following LRAST treatment alone, an increased D5-melanoma specific IFN-g release from TVDLN was observed (577 pg/ml; Fig. 4, A). While the administration of MDSC depleting antibodies (RB6-8C5) alone did not have any detectable effect on cytokine-release with any tumor cell-line, we observed a remarkable increase in the D5 tumor-specific IFN-g secretion from TVDLN in mice treated with the combination of LRAST and RB6-8C5 mAb (8193 pg/ml; Fig. 4, A).

Tumor growth was recorded starting 7 days after onset of the treatment. Compared to the control group both, LRAST and LRAST + RB6-8C5 led to a delay in tumor progression (Fig. 4, B). Within the first two weeks after treatment initiation tumor sizes of animals treated with the combination of LRAST and MDSC-depletion were significantly smaller than with LRAST alone (Fig. 4, B).

Use of RB6-8C5 leads to alteration of memory $CD8^+$ T cells

Effects of a lymphodepleting preconditioning with cyclophosphamid and the administration of antibodies targeting Gr-1 epitopes on $CD8^+$ cells and subsets thereof have already been investigated and will be discussed below (11, 44, 45). In the treatment groups containing lymphodepletion with cyclophosphamide, frequencies of $CD8^+$ cells increased during recovery from cyclophosphamide, followed by a reduction below the baseline and the values of control groups (RB6-8C5 alone and Isotype, Fig. 5A). RB6-8C5 treatment had no significant impact on the frequency of $CD8^+$ cells compared to untreated mice (Isotype group, Fig. 5A). Regarding the administration of MDSC depleting antibodies (anti-Gr-1 mAb, RB6-8C5) Matsuzaki *et al.* showed that the Gr-1 epitope is not only attributed to neutrophils and a subset of mouse DC, but is also expressed on memory type $CD8^+$ T cells (45). In the present investigation we confirmed the expression of the Gr-1-epitope on $CD8^+$ T cells, but not on $CD4^+$ T cells of female C57BL/6 mice (Fig. 5B and data not shown). The use of RB6-8C5 for MDSC-depletion as described above also led to a reduction in frequencies of $CD8^+$ $CD44^{high}$ $CD62L^+$ “central” and $CD8^+$ $CD44^{high}$ $CD62L^-$ “effector” memory cells (Fig. 5C). To address to which extent $Gr\text{-}1^+$ $CD8^+$ cells are affected by RB6-8C5 administration, we stained peripheral $CD45.2^+$ blood cells for the indicated markers.

In groups which included MDSC-depletion consistently lower proportions of Gr-1$^+$ CD8$^+$ central and effector memory cells were observed compared to the control group. To evaluate whether CD8$^+$ memory cells were depleted and not simply masked by cell bound RB6-8C5, we assessed their percentage of peripheral leukocytes. Interestingly, while CD8$^+$ central memory cells were consistently reduced in groups with RB6-8C5 administration, the portion of CD8$^+$ memory effectors in mice with LRAST + RB6-8C5 treatment steadily increased over 7 days following an initial decline after initiation of MDSC-depletion. This resulted in an increasing T_{em}:T_{cm}-ratio over time (Fig. 5D). On day 7 frequencies of CD8$^+$ effector memory cells from mice treated with LRAST + RB6-8C5 surpassed both control groups. Similar cell kinetics were not found in mice treated with lymphodepletion but without vaccination, followed by MDSC-depletion (LR + RB6-8C5). Thus, we conclude that administration of a whole cell vaccine after lymphodepleting preconditioning drives the expansion of CD8$^+$ memory cells with an effector phenotype (CD62L downregulation).

Discussion

The recent success of immune checkpoint-inhibition in the therapy of malignant melanoma and various other cancer entities emphasizes the significance of tumor-reactive cells, especially effector T cells (28, 46). However, tumors escape immune surveillance acquiring different accesses, including reduction of immune recognition and immune activation, developing resistance to immune effector mechanisms and establishing an immunosuppressive tumor microenvironment (47). As far as the latter is concerned MDSC were shown to be key mediators of immunosuppression in the tumor microenvironment, facilitating tumor outgrowth, metastasis, and negatively influencing the efficacy of immunotherapy of cancer (48–54).

In our experiments using a murine melanoma model we applied a combined immunotherapeutic approach, LRAST, consisting of lymphodepletion with the alkylating agent cyclophosphamide, followed by i.v. reconstitution with naive congenic spleen cells and active-specific tumor vaccination using GM-CSF-secreting whole tumor cells. In the poorly immunogenic D5-melanoma model we intended to improve T cell immunization at different levels simultaneously (55). Induction of a lymphopenic environment should empower T cells with a homeostatic drive to proliferate and, by simultaneous exposure to tumor-antigens via whole cell vaccine, ensure that preferentially tumor-directed T cells colonize empty lymphatic niches (56). GM-CSF is a hematopoietic cytokine and is often used as an adjuvant in immunotherapeutic regimes, especially vaccination strategies (57–60). It acts to promote the local recruitment of antigen-presenting cells and improves their maturation, thus enhancing antigen-presentation to T cells in TVDLN (61).

In line with previous reports (7, 56), we observed a remarkable increase in frequencies of CD11b$^+$ Ly6C^{high} Ly6G$^-$ (phenotype of M-MDSC) and CD11b$^+$ Ly6C$^+$ Ly6G$^+$ (phenotype of PMN-MDSC) cells (together also attributable as CD11b$^+$ Gr-1$^+$ cells) following LRAST. Within 24 days after lymphodepletion with 4,0 mg i.p. cylophosphamide per animal, PMN- as well as M-MDSC increased, peaking at day 7 in peripheral

blood and day 10 in spleen. Similar cell kinetics were reported by Salem *et al.* in blood, spleen and bone marrow of C57BL/6 mice after treatment with the same amount of i.p. cyclophosphamide (62). Although we observed $CD45.1^+$ cells of the myeloid lineage ($CD45.1^+$ $CD11b^+$) in the blood, spleen and tumor, reconstituted cells, in contrast to their host counterparts, did not give rise to relevant amounts of progeny with the phenotype of PMN- or M-MDSC or displayed a similar behavior in frequency kinetics over time. Thus, we conclude that $CD45.1^+$ MDSC do not contribute considerably to an immunosuppressive tumor micromilieu in mice with established D5 melanoma.

To enhance priming of tumor-specific T cells and anti-tumor effects of cytotoxic T cells we aimed to deplete $CD11b^+$ $Gr\text{-}1^+$ cells. Anti-Gr-1 mAb (clone: RB6-8C5) has already successfully been used to eliminate MDSC in tumor, spleen, peripheral blood and bone marrow of tumor-bearing and control mice (21, 23, 40–42). Thus, proof of principle for the efficacy of the anti-Gr-1 antibody and its therapeutic effect slowing down the growth of malignant tumors has already been brought forward. Srivastava *et al.*, for example, used 200 µg anti-Gr-1 mAb (RB6-8C5) every other day for a total amount of 4 weeks in a model of 3LL-lung carcinoma, starting one week after tumor inoculation. They observed a reduction of $CD11b^+$ $Gr\text{-}1^+$ in blood, spleen, bone marrow and tumor and also a significant reduction in tumor volume and weight (23). Using a similar approach in mice carrying 3LL-tumors, Zhang *et al.* were able to significantly reduce tumor-infiltrating MDSC, slowing down tumor growth and improving survival of the animals, using repeated i.p. administrations of 250 µg RB6-8C5, every 3 days starting 2 weeks after tumor inoculation (41).

In our experiments, we administered 230 µg anti-Gr-1 mAb (RB6-8C5) or isotope control via intraperitoneal injection every other day, starting with the day of cyclophosphamide administration and continuing until the animals were euthanized, thus ensuring the period of RB6-8C5 administration would cover the days with maximum MDSC frequencies. To maintain comparability, dose and time intervals between the single doses of antibody were set in accordance to previous reports (22, 41). However, assessing the depletion status of MDSC is not trivial since fluorochrome labelled Ly6G antibodies (clone 1A8), which we and others used to distinguish between PMN- and M-MDSC, do not bind due to the same binding site, when anti-Gr-1 antibodies were administered previously (21, 22, 24). Thus, we performed co-staining and quantification of RB6-8C5-bound cells using a secondary antibody-approach with fluorochrome-labeled antibodies directed against goat-IgG heavy chains of the anti-Gr-1 antibodies (21, 22, 24, 45). Complete absence of MDSC after conventional and secondary antibody staining indicated that MDSC were reliably depleted. Absence of MDSC regarding the conventional staining, but detection of secondary Ab positive cells in the same gate or neighboring areas, indicated the persistence of MDSC. Noteworthy, in some cases, we observed, (a) secondary Ab bound cells negatively stained for Ly6G, (b) a cell cloud with a positive and negative portion regarding Ly6G-staining, or (c) secondary Ab bound cells within the PMN-gate. The fact, that cells of all three cases retained the same Ly6C intensity suggests that in every case PMN-MDSC with different degrees of Gr-1 epitope saturation with RB6-8C5 were visualized. Hence, the absence of PMN-MDSC in their designated gate was not necessarily accompanied with complete absence or depletion of PMN-MDSC.

This in mind, we observed a successful depletion of PMN-MDSC in the peripheral blood, 2 and 4 days after treatment initiation, as there were no secondary antibody-bound cells in the PMN-gate or neighboring areas. In contrast, the frequencies of M-MDSC appeared to be reduced, but not completely depleted. In the time-span, when maximum frequencies of MDSC were to be expected following LRAST treatment (day 7 and day 10), frequencies of PMN-MDSC appeared to be significantly reduced, but, at the same time, a major portion of cells in the PMN-gate showed secondary Ab binding. Since anti-Gr-1 antibodies (RB6-8C5) were shown to persist on the cell surface of MDSC for up to 4 days and might retain suppressive activity (21, 22), the persisting portion of RB6-8C5-bound cells might represent an obstacle to therapy due to preserved immunosuppressive properties. Therefore, we aimed at investigating whether the observed reduction of PMN-MDSC, despite the occurrence of RB6-8C5-bound cells, would be sufficient to improve a tumor-specific T cell response and display a measurable therapeutic effect.

IFN-γ secretion is often used as a marker for the cytotoxic properties of T cells, including anti-tumor reactivity (63–66). Van den Engel *et al.* have already demonstrated an increase in IFN-γ secretion from TVDLN after LRAST (7). Here, we hypothesized that tumor-specific T cells in TVDLN from mice in the group with LRAST + RB6-8C5 treatment would exert improved IFN-γ producing capability due to better T cell-priming after MDSC-depletion. TVDLN from mice treated with LRAST alone already presented an increased tumor specific IFN-γ production and a delay in tumor outgrow compared to untreated mice. We could show that RB6-8C5 administration in addition to LRAST could further increase the IFN-γ-secretion from TVDLN, though significant results could not be obtained due to the variability of results per mouse. In accordance to that, tumor growth in mice treated with LRAST + RB6-8C5 appeared significantly reduced in the initial treatment phase up to 13 days after tumor inoculation, including the point in time with maximum IFN-γ secretion and covering the timespan of successful MDSC-depletion in our experiments - at least regarding PMN-MDSC. Since PMN-MDSC are known to mainly target T cell priming accounting for tumor-specific T cell tolerance (20), the improvement in tumor-specific INF-γ secretion from TVDLN and the delay of tumor-growth which is chronologically fitting to the time-span of successful reduction of PMN-MDSC, implies that the observed effects in fact are attributable to the administration of MDSC depleting antibodies. In contrast to Srivastava *et al.* and Zhang *et al.* (23, 41), who gained good long-term results due to a presumably successful long-term depletion of MDSC in their tumor models, our results clearly demonstrate the recurrence of MDSC, especially the PMN-subset after repetitive administration of anti-Gr-1 antibodies. Interestingly, the presence of RB6-8C5-bound cells, as indicated by secondary Ab binding, initially increased over time. After approximately 4 weeks of repetitive RB6-8C5-administration binding of depleting antibodies could not be observed anymore and MDSC depletion appeared insufficient. It is noteworthy though, that the comparability of our data to pre-existing literature on MDSC-depletion using RB6-8C5 is impaired due to a pervasive pre-treatment, which even bears the risk to be a MDSC driving stimulus itself. We assume that most likely side effects of the components of LRAST work in synergy and oppose MDSC eradication. Hence, despite its positive immunomodulating features, low-dose cyclophosphamide is known to increase levels of various cytokines (GM-CSF, IL-1b, IL-5, IL-10, IFN-γ, TNF-α) which can contribute to the expansion and activation of MDSC (67). GM-CSF, a major component within LRAST, and in turn a driving force in MDSC recruitment. It is not only found manifold as an

adjuvant in immunotherapeutic regimes, but also produced by many human and murine tumor cell lines (68). GM-CSF has been shown to recruit MDSC into secondary lymphoid tissues with a consecutively impaired function of tumor-specific $CD8^+$ T cells (38). In experiments with irradiated GM-CSF producing B78H1-GM cells, a cell line derived from the B16 melanoma, Serafini *et al.* proposed a cut-off concentration at 1500 ng / 10^6 cells / 24 hours, which – if exceeded – was associated with a suppression of antigen-specific T cell response (69). Irradiated D5G6 cells used in this work showed an *in vitro* GM-CSF production of 154 ng / 10^6 cells / 24 hours with an ascending tendency over 6 days (data not shown). Although, the GM-CSF concentrations observed in our experiments are below the proposed cut-off. A positive contribution to MDSC recruitment by GM-CSF cannot be ruled out, especially considering the potentially synergistic effects when combined with cyclophosphamide. Furthermore, even the anti-Gr-1 depleting antibodies themselves may act as a driver for MDSC expansion and thereby stand in the way of their own therapeutic purpose. Single application of RB6-8C5 was shown to be accompanied by enlarged spleens with increased cell numbers 9 days after antibody injection (40); observations which we also could obtain in our experiments. An increase in numbers of PMN- and M-MDSC was attributed to a pronounced proliferative stimulus on early myeloid precursors due to depletion (40). More to the point, following repetitive administration of RB6-8C5 every other day, Ribechini *et al.* found an induction of STAT1, STAT3 and STAT5. STAT3 in particular acts as an inducer of myeloid cell lineages and thereby may promote MDSC differentiation and activation (22).

Overall, the increasing frequencies of PMN-MDSC despite administration of anti-Gr-1 mAb on the one hand, and an increasing number of cells with cell-bound RB6-8C5 on the other, indicate that antibody administration becomes insufficient in keeping up with the reproduction / regeneration of MDSC, especially the PMN-subset. The abrogated depleting efficacy of long-term use of RB6-8C5 together with the fact, that, in the long run, no RB6-8C5 bound cells were detectable in the gates of both MDSC-subsets, implies the existence of a neutralizing mechanism (e.g. neutralizing self-antibodies) directed against RB6-8C5 antibodies.

Depending on the tissue localization the ratio of MDSC subpopulations and their suppressive activity vary, as does their susceptibility to RB6-8C5 (13). Overall, we observed a differing behavior of the M-MDSC subset compared to their PMN counterparts in response to MDSC depletion. For a period of 4 weeks, repetitive RB6-8C5 administration did not – apart from an initial reduction in peripheral blood - have any significant depleting effect on M-MDSC in the peripheral blood of tumor bearing mice. In previous reports particularly tumor-localized M-MDSC were shown to be resistant to depletion with anti-Gr-1 mAb and the frequency of $Ly6C^{high}$ cells was not altered 48 hours after a single administration of 250 µg RB6-8C5 (22, 70). Although we did not evaluate the efficacy of RB6-8C5 regarding M-MDSC depletion within the tumor tissue, we expect a similar resistance. Still, given the initial occurrence of RB6-8C5 bound cells in the M-MDSC gate and a short-term reduction in numbers of M-MDSC after treatment initiation with LRAST + RB6-8C5, we cannot assume a general resistance of M-MDSC to anti-Gr-1 mAbs. However, M-MDSC frequency kinetics appeared to be independent of anti-Gr-1 Ab administration. This has to be evaluated in future experiments.

Apart from the MDSC-depleting properties of anti-Gr-1 antibodies, a secondary focus was to elucidate the effect of RB6-8C5 on $CD8^+$ cells and $CD8^+$ memory T cell subsets (T_{cm} and T_{em}) in mice after LRAST treatment. Both, the anti-Gr-1 antibodies as well as lymphopenia induced by cyclophosphamide provably have an impact on $CD8^+$ T cells and their memory subsets (11, 44, 45), but - as to our knowledge - the combined effect has not been investigated so far. In line with previous work by Matsuzaki *et al.*, we confirmed the expression of Gr-1 on memory $CD8^+$, but not $CD4^+$ T cells with FACS analysis (data not shown) and observed a depletion of $CD8^+$ memory T cell subsets following RB6-8C5 administration (45). In accordance to results from Salem *et al.* the relative cell frequency kinetics of $CD8^+$ cells were obviously influenced by lymphopenia / lymphopenia driven homeostatic proliferation (62), but no significant impact of MDSC depletion on the population of $CD8^+$ cells could be observed. However, looking at the $CD8^+$ memory subsets (T_{cm} and T_{em}), reduced staining capability with fluorochrome-conjugated mAb directed towards Gr-1 and reduced overall frequencies indicated that not only targeting of memory T cells by anti-Gr-1 mAb occurred, but in fact a portion of both memory T cell subsets was depleted following RB6-8C5 administration, independent from pretreatment with LRAST. Nevertheless, despite of continuous injections with anti-Gr-1 mAb, we observed that frequencies of T_{em}, more than T_{cm}, in the peripheral blood strongly increased following LRAST, reflecting in a T_{em}:T_{cm} ratio of 3.5:1 by day 7, compared to a ratio of 1.2:1 in the control group. T_{em} in mice with RB6-8C5 monotherapy and LR + RB6-8C5 treatment (no vaccination) remained reduced in the same period of time. These results go in line with observations from Ma and coworkers. They found that the exposure to a tumor vaccine during homeostatic recovery after induction of lymphopenia resulted in strong expansion of $CD4^+$ and $CD8^+$ $CD44^{high}$ $CD62L^{low}$ effector memory T cells, accompanied by a pronounced tumor-specific IFN-γ production and better tumor reactivity (11). In our experiments the proliferative drive seems to exceed the depleting properties of the anti-Gr-1 antibodies exerted upon the Gr-1 expressing $CD8^+$ memory T cells which are capable of producing significant amounts of IFN-γ in a tumor-specific manner (11, 45). Nevertheless, it remains to be evaluated whether the observed increase in IFN-γ secretion from TVDLN is attributable to the increased occurrence of T_{em}, since these cells lack the ability to home lymphatic tissue (33). Although, compared to $CD8^+$ $T_{em,}$ $CD8^+$ T_{cm} are referred to as the cell population with a more pronounced role in antitumor-immunity. Downregulation of CD62L enables T_{em} to quickly migrate to peripheral tissues and exert effector functions upon antigen encounter (35). Thus T_{em} might successfully invade tumor tissue and kill transformed cells. We therefore hypothesize that the increased frequencies of T_{em} cells might be reflected in the initial delay of tumor growth of mice treated with LRAST + RB6-8C5. Nevertheless, the influence of RB6-8C5 on the $CD8^+$ memory T cell compartment might limit the anti-tumor efficacy of LRAST + RB6-8C5 treatment, to provide suitable data that can be translated into improved patient care.

Conclusion

Overall, within the wide field of immunotherapy of cancer combination therapies continue to be promising. With LRAST, a therapy combing lymphodepletion with active-specific tumor cell vaccination, we could confirm pre-existing results showing a notable delay in melanoma growth. By adding the use of

monoclonal depleting antibodies (anti-Gr-1 mAb) our data highlight the significance of MDSC as major tumor promoting cells, as depletion of MDSC further delayed tumor progression and improved the tumor specific IFN-γ response. Nevertheless, the positive effects of MDSC depletion in addition to LRAST were mainly restricted to the PMN subset and the first weeks after treatment initiation. The recurrence of PMN-MDSC and the impact of anti-Gr-1 depleting antibodies on the memory T cell compartment, might be responsible for the failure in long-term tumor reduction. Overall, we could show that reduction of the frequencies of MDSC in animals with established melanoma has beneficial effects. Future experiments are required to further highlight cell dynamics and their significance on tumor growth within a combined immunotherapeutic approach.

List Of Abbreviations

Ab Antibody

DC dendritic cell

i.p. intraperitoneal

LRAST Lymphodepletion, Reconstitution and Active-Specific Tumor cell vaccination

mAb monoclonal antibody

MDSC Myeloid-derived suppressor cells

M-MDSC monocytic MDSC

PMN-MDSC polymorphonuclear MDSC

s.c. subcutaneous

T_{cm} central-memory T cell

T_{eff} effector T cell

T_{em} effector-memory T cell

Treg regulatory T cell

TVDLN tumor vaccine draining lymph nodes

Declarations

Ethics approval: The animal experiments were performed after approval by the local regulatory agency (Regierung von Oberbayern, Munich, Germany).

Consent for publication: Not applicable.

Availability of data and materials: The datasets used and/or analyzed during the current study are available from the corresponding author on reasonable request.

Competing interests: None declared.

Funding: German Center for Lung Research (DZL), Heidelberg, Germany. Chiles Foundation.

Authors´ Contributions: HW, NKE, and RAH conceived and supervised the study. PR performed all experiments. JRK contributed to conduction of experiments and interpretation of data. LB kindly provided depleting antibodies and control. All authors have contributed to writing, reviewing and editing, and have approved the final manuscript.

Acknowledgments: Not applicable.

References

1. Herzberg B, Fisher DE. Metastatic melanoma and immunotherapy. Clin Immunol. 2016;172:105-10.
2. Mattia G, Puglisi R, Ascione B, Malorni W, Care A, Matarrese P. Cell death-based treatments of melanoma:conventional treatments and new therapeutic strategies. Cell Death Dis. 2018;9(2):112.
3. Syn NL, Teng MWL, Mok TSK, Soo RA. De-novo and acquired resistance to immune checkpoint targeting. Lancet Oncol. 2017;18(12):e731-e41.
4. Hanna MG, Jr., Howard J, Vermorken J. Active specific immunotherapy: using tumor heterogeneity to successfully fight cancer. Hum Vaccin Immunother. 2014;10(11):3286-96.
5. Hu HM, Poehlein CH, Urba WJ, Fox BA. Development of antitumor immune responses in reconstituted lymphopenic hosts. Cancer Res. 2002;62(14):3914-9.
6. Machiels JP, Reilly RT, Emens LA, Ercolini AM, Lei RY, Weintraub D, et al. Cyclophosphamide, doxorubicin, and paclitaxel enhance the antitumor immune response of granulocyte/macrophage-colony stimulating factor-secreting whole-cell vaccines in HER-2/neu tolerized mice. Cancer Res. 2001;61(9):3689-97.
7. van den Engel NK, Ruttinger D, Rusan M, Kammerer R, Zimmermann W, Hatz RA, et al. Combination immunotherapy and active-specific tumor cell vaccination augments anti-cancer immunity in a mouse model of gastric cancer. J Transl Med. 2011;9:140.
8. Cho BK, Rao VP, Ge Q, Eisen HN, Chen J. Homeostasis-stimulated proliferation drives naive T cells to differentiate directly into memory T cells. J Exp Med. 2000;192(4):549-56.
9. Mackall CL, Hakim FT, Gress RE. Restoration of T-cell homeostasis after T-cell depletion. Semin Immunol. 1997;9(6):339-46.
10. Nowak AK, Lake RA, Robinson BW. Combined chemoimmunotherapy of solid tumours: improving vaccines? Adv Drug Deliv Rev. 2006;58(8):975-90.

11. Ma J, Urba WJ, Si L, Wang Y, Fox BA, Hu HM. Anti-tumor T cell response and protective immunity in mice that received sublethal irradiation and immune reconstitution. Eur J Immunol. 2003;33(8):2123-32.
12. van der Burg SH, Arens R, Ossendorp F, van Hall T, Melief CJ. Vaccines for established cancer: overcoming the challenges posed by immune evasion. Nat Rev Cancer. 2016;16(4):219-33.
13. Kumar V, Patel S, Tcyganov E, Gabrilovich DI. The Nature of Myeloid-Derived Suppressor Cells in the Tumor Microenvironment. Trends Immunol. 2016;37(3):208-20.
14. Gabrilovich DI, Nagaraj S. Myeloid-derived suppressor cells as regulators of the immune system. Nat Rev Immunol. 2009;9(3):162-74.
15. de Haas N, de Koning C, Spilgies L, de Vries IJ, Hato SV. Improving cancer immunotherapy by targeting the STATe of MDSCs. Oncoimmunology. 2016;5(7):e1196312.
16. Movahedi K, Guilliams M, Van den Bossche J, Van den Bergh R, Gysemans C, Beschin A, et al. Identification of discrete tumor-induced myeloid-derived suppressor cell subpopulations with distinct T cell-suppressive activity. Blood. 2008;111(8):4233-44.
17. Youn JI, Nagaraj S, Collazo M, Gabrilovich DI. Subsets of myeloid-derived suppressor cells in tumor-bearing mice. J Immunol. 2008;181(8):5791-802.
18. Veglia F, Perego M, Gabrilovich D. Myeloid-derived suppressor cells coming of age. Nat Immunol. 2018;19(2):108-19.
19. Wada S, Yoshimura K, Hipkiss EL, Harris TJ, Yen HR, Goldberg MV, et al. Cyclophosphamide augments antitumor immunity: studies in an autochthonous prostate cancer model. Cancer Res. 2009;69(10):4309-18.
20. Gabrilovich DI. Myeloid-Derived Suppressor Cells. Cancer Immunol Res. 2017;5(1):3-8.
21. Ma C, Kapanadze T, Gamrekelashvili J, Manns MP, Korangy F, Greten TF. Anti-Gr-1 antibody depletion fails to eliminate hepatic myeloid-derived suppressor cells in tumor-bearing mice. J Leukoc Biol. 2012;92(6):1199-206.
22. Ribechini E, Leenen PJ, Lutz MB. Gr-1 antibody induces STAT signaling, macrophage marker expression and abrogation of myeloid-derived suppressor cell activity in BM cells. Eur J Immunol. 2009;39(12):3538-51.
23. Srivastava MK, Zhu L, Harris-White M, Kar UK, Huang M, Johnson MF, et al. Myeloid suppressor cell depletion augments antitumor activity in lung cancer. PLoS One. 2012;7(7):e40677.
24. Ma C, Greten TF. Editorial: "Invisible" MDSC in tumor-bearing individuals after antibody depletion: fact or fiction? J Leukoc Biol. 2016;99(6):794.
25. Barnes TA, Amir E. HYPE or HOPE: the prognostic value of infiltrating immune cells in cancer. Br J Cancer. 2017;117(4):451-60.
26. Fridman WH, Pages F, Sautes-Fridman C, Galon J. The immune contexture in human tumours: impact on clinical outcome. Nat Rev Cancer. 2012;12(4):298-306.

27. Gooden MJ, de Bock GH, Leffers N, Daemen T, Nijman HW. The prognostic influence of tumour-infiltrating lymphocytes in cancer: a systematic review with meta-analysis. Br J Cancer. 2011;105(1):93-103.
28. Reiser J, Banerjee A. Effector, Memory, and Dysfunctional CD8(+) T Cell Fates in the Antitumor Immune Response. J Immunol Res. 2016;2016:8941260.
29. Abu Eid R, Ahmad S, Lin Y, Webb M, Berrong Z, Shrimali R, et al. Enhanced Therapeutic Efficacy and Memory of Tumor-Specific CD8 T Cells by Ex Vivo PI3K-delta Inhibition. Cancer Res. 2017;77(15):4135-45.
30. Abu Eid R, Friedman KM, Mkrtichyan M, Walens A, King W, Janik J, et al. Akt1 and -2 inhibition diminishes terminal differentiation and enhances central memory CD8(+) T-cell proliferation and survival. Oncoimmunology. 2015;4(5):e1005448.
31. van der Waart AB, van de Weem NM, Maas F, Kramer CS, Kester MG, Falkenburg JH, et al. Inhibition of Akt signaling promotes the generation of superior tumor-reactive T cells for adoptive immunotherapy. Blood. 2014;124(23):3490-500.
32. Wu F, Zhang W, Shao H, Bo H, Shen H, Li J, et al. Human effector T cells derived from central memory cells rather than CD8(+)T cells modified by tumor-specific TCR gene transfer possess superior traits for adoptive immunotherapy. Cancer Lett. 2013;339(2):195-207.
33. Nolz JC. Molecular mechanisms of CD8(+) T cell trafficking and localization. Cell Mol Life Sci. 2015;72(13):2461-73.
34. Reading JL, Galvez-Cancino F, Swanton C, Lladser A, Peggs KS, Quezada SA. The function and dysfunction of memory CD8(+) T cells in tumor immunity. Immunol Rev. 2018;283(1):194-212.
35. Klebanoff CA, Gattinoni L, Torabi-Parizi P, Kerstann K, Cardones AR, Finkelstein SE, et al. Central memory self/tumor-reactive CD8+ T cells confer superior antitumor immunity compared with effector memory T cells. Proc Natl Acad Sci U S A. 2005;102(27):9571-6.
36. Hu HM, Urba WJ, Fox BA. Gene-modified tumor vaccine with therapeutic potential shifts tumor-specific T cell response from a type 2 to a type 1 cytokine profile. J Immunol. 1998;161(6):3033-41.
37. Poehlein CH, Haley DP, Walker EB, Fox BA. Depletion of tumor-induced Treg prior to reconstitution rescues enhanced priming of tumor-specific, therapeutic effector T cells in lymphopenic hosts. Eur J Immunol. 2009;39(11):3121-33.
38. Nockel J, van den Engel NK, Winter H, Hatz RA, Zimmermann W, Kammerer R. Characterization of gastric adenocarcinoma cell lines established from CEA424/SV40 T antigen-transgenic mice with or without a human CEA transgene. BMC cancer. 2006;6:57.
39. Meijer SL, Dols A, Hu HM, Chu Y, Romero P, Urba WJ, et al. Reduced L-selectin (CD62LLow) expression identifies tumor-specific type 1 T cells from lymph nodes draining an autologous tumor cell vaccine. Cell Immunol. 2004;227(2):93-102.
40. Condamine T, Kumar V, Ramachandran IR, Youn JI, Celis E, Finnberg N, et al. ER stress regulates myeloid-derived suppressor cell fate through TRAIL-R-mediated apoptosis. J Clin Invest. 2014;124(6):2626-39.

41. Zhang Y, Liu Q, Zhang M, Yu Y, Liu X, Cao X. Fas signal promotes lung cancer growth by recruiting myeloid-derived suppressor cells via cancer cell-derived PGE2. J Immunol. 2009;182(6):3801-8.
42. Hurez V, Daniel BJ, Sun L, Liu AJ, Ludwig SM, Kious MJ, et al. Mitigating age-related immune dysfunction heightens the efficacy of tumor immunotherapy in aged mice. Cancer Res. 2012;72(8):2089-99.
43. Srivastava MK, Zhu L, Harris-White M, Huang M, St John M, Lee JM, et al. Targeting myeloid-derived suppressor cells augments antitumor activity against lung cancer. Immunotargets Ther. 2012;2012(1):7-12.
44. Salem ML, Diaz-Montero CM, Al-Khami AA, El-Naggar SA, Naga O, Montero AJ, et al. Recovery from cyclophosphamide-induced lymphopenia results in expansion of immature dendritic cells which can mediate enhanced prime-boost vaccination antitumor responses in vivo when stimulated with the TLR3 agonist poly(I:C). J Immunol. 2009;182(4):2030-40.
45. Matsuzaki J, Tsuji T, Chamoto K, Takeshima T, Sendo F, Nishimura T. Successful elimination of memory-type CD8+ T cell subsets by the administration of anti-Gr-1 monoclonal antibody in vivo. Cell Immunol. 2003;224(2):98-105.
46. Durgeau A, Virk Y, Corgnac S, Mami-Chouaib F. Recent Advances in Targeting CD8 T-Cell Immunity for More Effective Cancer Immunotherapy. Front Immunol. 2018;9:14.
47. Teng MW, Galon J, Fridman WH, Smyth MJ. From mice to humans: developments in cancer immunoediting. J Clin Invest. 2015;125(9):3338-46.
48. Umansky V, Blattner C, Fleming V, Hu X, Gebhardt C, Altevogt P, et al. Myeloid-derived suppressor cells and tumor escape from immune surveillance. Semin Immunopathol. 2017;39(3):295-305.
49. Chesney JA, Mitchell RA, Yaddanapudi K. Myeloid-derived suppressor cells-a new therapeutic target to overcome resistance to cancer immunotherapy. J Leukoc Biol. 2017;102(3):727-40.
50. Gebhardt C, Sevko A, Jiang H, Lichtenberger R, Reith M, Tarnanidis K, et al. Myeloid Cells and Related Chronic Inflammatory Factors as Novel Predictive Markers in Melanoma Treatment with Ipilimumab. Clin Cancer Res. 2015;21(24):5453-9.
51. Hansen GL, Gaudernack G, Brunsvig PF, Cvancarova M, Kyte JA. Immunological factors influencing clinical outcome in lung cancer patients after telomerase peptide vaccination. Cancer Immunol Immunother. 2015;64(12):1609-21.
52. Limagne E, Euvrard R, Thibaudin M, Rebe C, Derangere V, Chevriaux A, et al. Accumulation of MDSC and Th17 Cells in Patients with Metastatic Colorectal Cancer Predicts the Efficacy of a FOLFOX-Bevacizumab Drug Treatment Regimen. Cancer Res. 2016;76(18):5241-52.
53. Martens A, Wistuba-Hamprecht K, Geukes Foppen M, Yuan J, Postow MA, Wong P, et al. Baseline Peripheral Blood Biomarkers Associated with Clinical Outcome of Advanced Melanoma Patients Treated with Ipilimumab. Clin Cancer Res. 2016;22(12):2908-18.
54. Weber R, Fleming V, Hu X, Nagibin V, Groth C, Altevogt P, et al. Myeloid-Derived Suppressor Cells Hinder the Anti-Cancer Activity of Immune Checkpoint Inhibitors. Front Immunol. 2018;9:1310.

55. Arca MJ, Krauss JC, Strome SE, Cameron MJ, Chang AE. Diverse manifestations of tumorigenicity and immunogenicity displayed by the poorly immunogenic B16-BL6 melanoma transduced with cytokine genes. Cancer Immunol Immunother. 1996;42(4):237-45.
56. Salem ML, Kadima AN, El-Naggar SA, Rubinstein MP, Chen Y, Gillanders WE, et al. Defining the ability of cyclophosphamide preconditioning to enhance the antigen-specific CD8+ T-cell response to peptide vaccination: creation of a beneficial host microenvironment involving type I IFNs and myeloid cells. J Immunother. 2007;30(1):40-53.
57. Dranoff G, Jaffee E, Lazenby A, Golumbek P, Levitsky H, Brose K, et al. Vaccination with irradiated tumor cells engineered to secrete murine granulocyte-macrophage colony-stimulating factor stimulates potent, specific, and long-lasting anti-tumor immunity. Proc Natl Acad Sci U S A. 1993;90(8):3539-43.
58. Dunussi-Joannopoulos K, Dranoff G, Weinstein HJ, Ferrara JL, Bierer BE, Croop JM. Gene immunotherapy in murine acute myeloid leukemia: granulocyte-macrophage colony-stimulating factor tumor cell vaccines elicit more potent antitumor immunity compared with B7 family and other cytokine vaccines. Blood. 1998;91(1):222-30.
59. Kaufman HL, Ruby CE, Hughes T, Slingluff CL, Jr. Current status of granulocyte-macrophage colony-stimulating factor in the immunotherapy of melanoma. J Immunother Cancer. 2014;2:11.
60. Vieweg J, Rosenthal FM, Bannerji R, Heston WD, Fair WR, Gansbacher B, et al. Immunotherapy of prostate cancer in the Dunning rat model: use of cytokine gene modified tumor vaccines. Cancer Res. 1994;54(7):1760-5.
61. Parmiani G, Castelli C, Pilla L, Santinami M, Colombo MP, Rivoltini L. Opposite immune functions of GM-CSF administered as vaccine adjuvant in cancer patients. Ann Oncol. 2007;18(2):226-32.
62. Salem ML, Al-Khami AA, El-Nagaar SA, Zidan AA, Al-Sharkawi IM, Marcela Diaz-Montero C, et al. Kinetics of rebounding of lymphoid and myeloid cells in mouse peripheral blood, spleen and bone marrow after treatment with cyclophosphamide. Cell Immunol. 2012;276(1-2):67-74.
63. Kline J, Zhang L, Battaglia L, Cohen KS, Gajewski TF. Cellular and molecular requirements for rejection of B16 melanoma in the setting of regulatory T cell depletion and homeostatic proliferation. J Immunol. 2012;188(6):2630-42.
64. Bhat P, Leggatt G, Waterhouse N, Frazer IH. Interferon-gamma derived from cytotoxic lymphocytes directly enhances their motility and cytotoxicity. Cell Death Dis. 2017;8(6):e2836.
65. Gerber SA, Sedlacek AL, Cron KR, Murphy SP, Frelinger JG, Lord EM. IFN-gamma mediates the antitumor effects of radiation therapy in a murine colon tumor. Am J Pathol. 2013;182(6):2345-54.
66. Lee S, Margolin K. Cytokines in cancer immunotherapy. Cancers (Basel). 2011;3(4):3856-93.
67. Peter S, Bak G, Hart K, Berwin B. Ovarian tumor-induced T cell suppression is alleviated by vascular leukocyte depletion. Transl Oncol. 2009;2(4):291-9.
68. Mytar B, Stec M, Szatanek R, Weglarczyk K, Szewczyk K, Szczepanik A, et al. Characterization of human gastric adenocarcinoma cell lines established from peritoneal ascites. Oncol Lett. 2018;15(4):4849-58.

69. Serafini P, Carbley R, Noonan KA, Tan G, Bronte V, Borrello I. High-dose granulocyte-macrophage colony-stimulating factor-producing vaccines impair the immune response through the recruitment of myeloid suppressor cells. Cancer Res. 2004;64(17):6337-43.
70. Kumar V, Cheng P, Condamine T, Mony S, Languino LR, McCaffrey JC, et al. CD45 Phosphatase Inhibits STAT3 Transcription Factor Activity in Myeloid Cells and Promotes Tumor-Associated Macrophage Differentiation. Immunity. 2016;44(2):303-15.

Figures

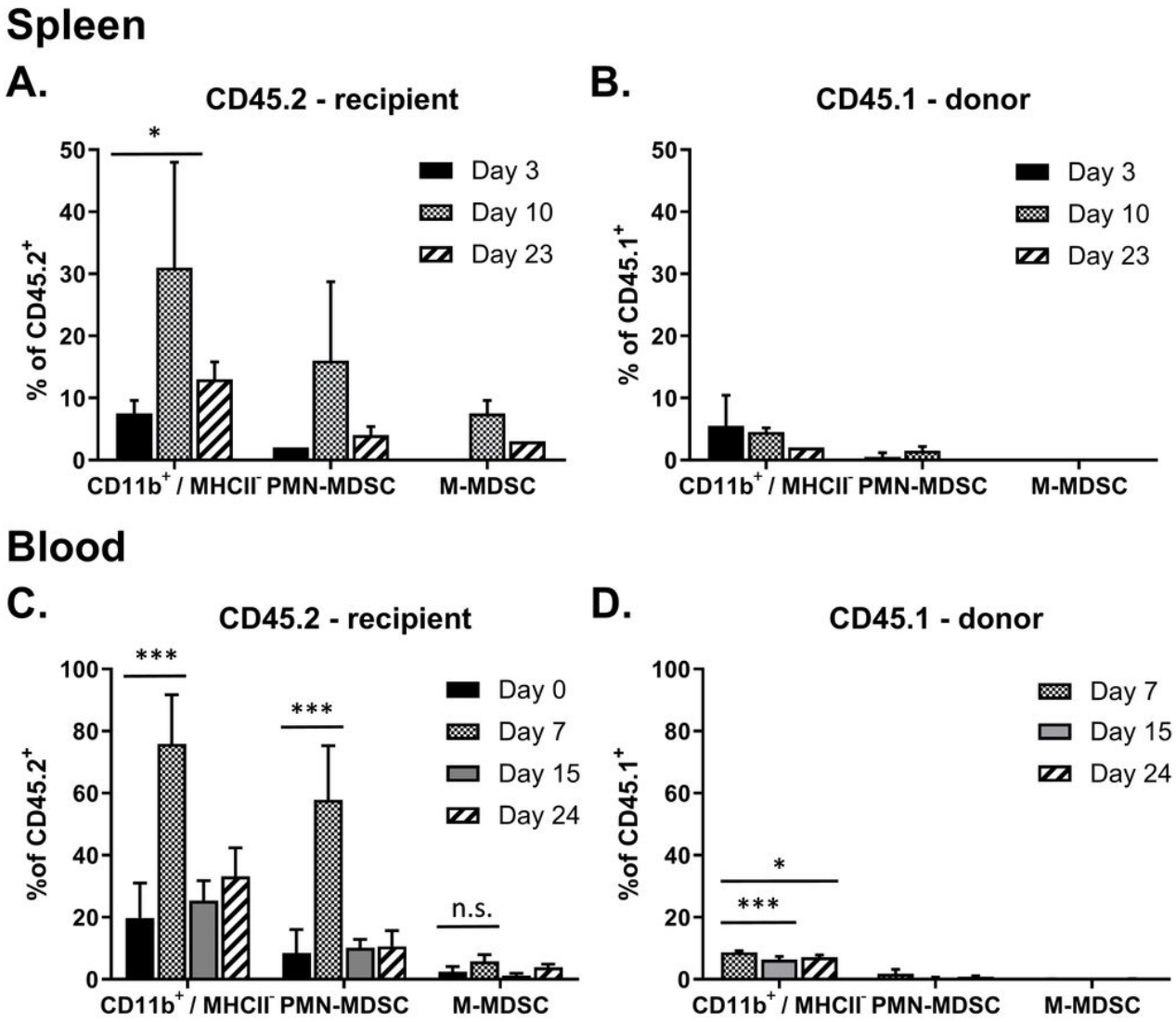

Figure 1

Myeloid cells from spleen and blood at different time points after LRAST-treatment. C57BL/6 mice were exposed to 5x104 D5-cells by s.c. injection and treated according to the LRAST scheme with cyclophosphamide (L) und active-specific vaccination (AST). CD11b+ MHC-II- cells, PMN-MDSC (CD11b+

Ly6G+ Ly6C+) and M-MDSC (CD11b+ Ly6G- Ly6Chigh) from A. + B. spleen (n = 2) und C. + D. blood (n = 3) were determined on days 3, 10 und 23 (spleen) and 0, 7, 15 und 24 (blood, except for CD45.1+ donor cells, which were not in situ of the recipient mice on day 0). Frequencies of the different myeloid cell types are depicted as percentages of CD45+ leucocytes and separated into CD45.2+ (recipient mouse, A. and C.) and CD45.1+ (donor mouse, B. and D.) cells, respectively.

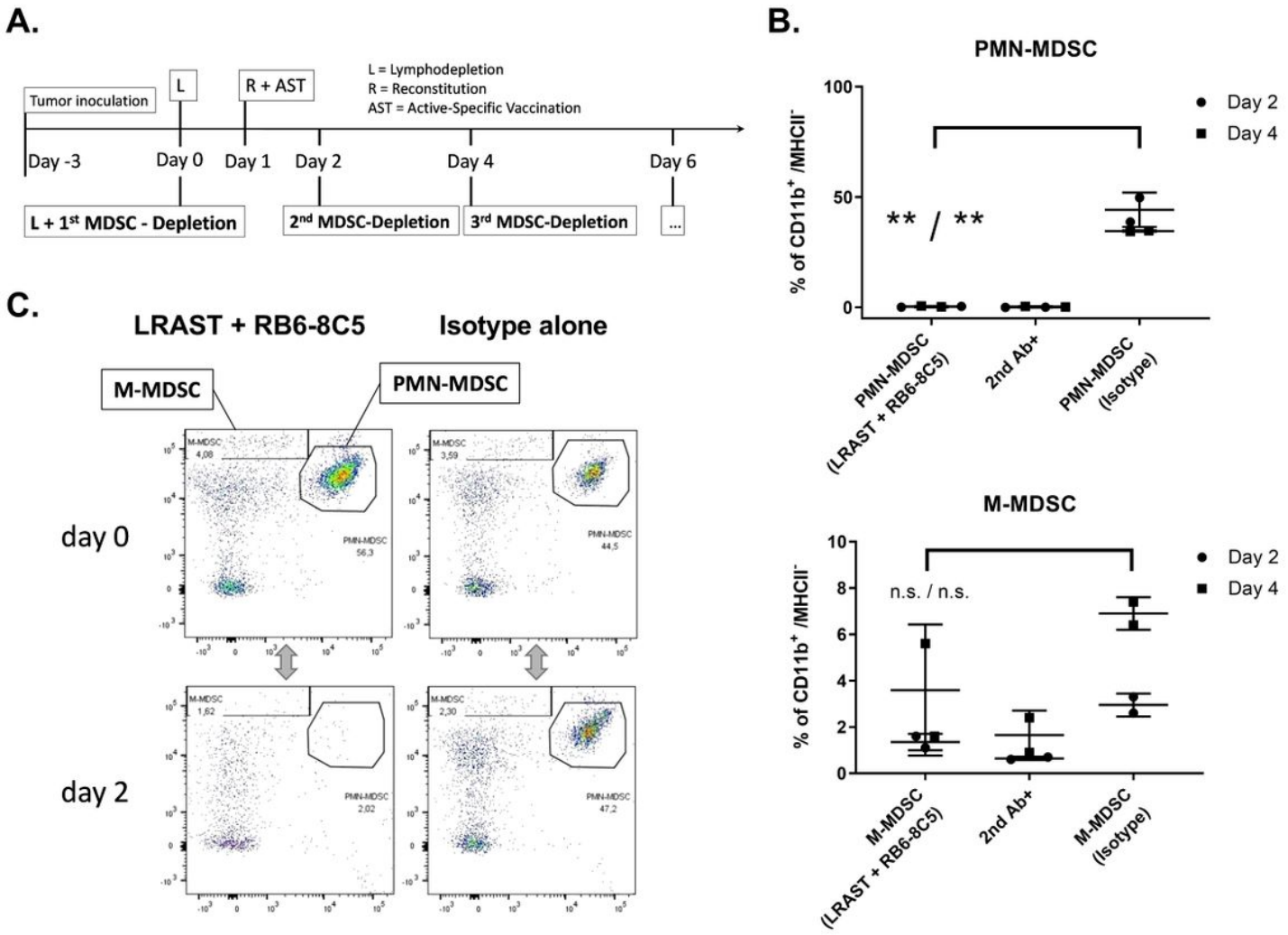

Figure 2

Successful elimination of PMN-MDSC in the initial treatment phase of LRAST + RB6-8C5. (A) LRAST treatment scheme. D5 tumor cells (5 x 104) were injected s.c. into C57BL6 mice 3 days prior to LRAST treatment. One day following lymphopenia induction with cyclophosphamide (200 mg/kg, i.p.) C57BL/6 (CD45.2+) mice were reconstituted i.v. with 20 × 106 splenocytes from naïve C57BL/6 (CD45.1+) mice and vaccinated s.c. with 10 x 106 irradiated D5G6 cells. Beginning on the day of lymphodepletion, in groups with MDSC depletion, mice received 230 µg anti-Gr-1 mAb (clone: RB6-8C5) i.p. every other day until mice were euthanized. (B) Plots depict mean and standard deviation visualizing depletion results assessed by flow cytometry for PMN-MDSC and M-MDSC on days 2 and 4 from the blood of mice treated with LRAST + RB6-8C5 compared to control (Isotype alone), respectively. Results in the middle of both

plots represent % of CD11b+/MHCII- cells with RB6-8C5-binding as indicated by secondary antibody staining (“2nd Ab+”). (C) Representative dot plots for (B). Dot plots demonstrate depletion of PMN- and M-MDSC on day 2 (= 48 hours) after treatment initiation with LRAST + RB6-8C5 treated mice compared to mice receiving Isotype control AB without any further treatment.

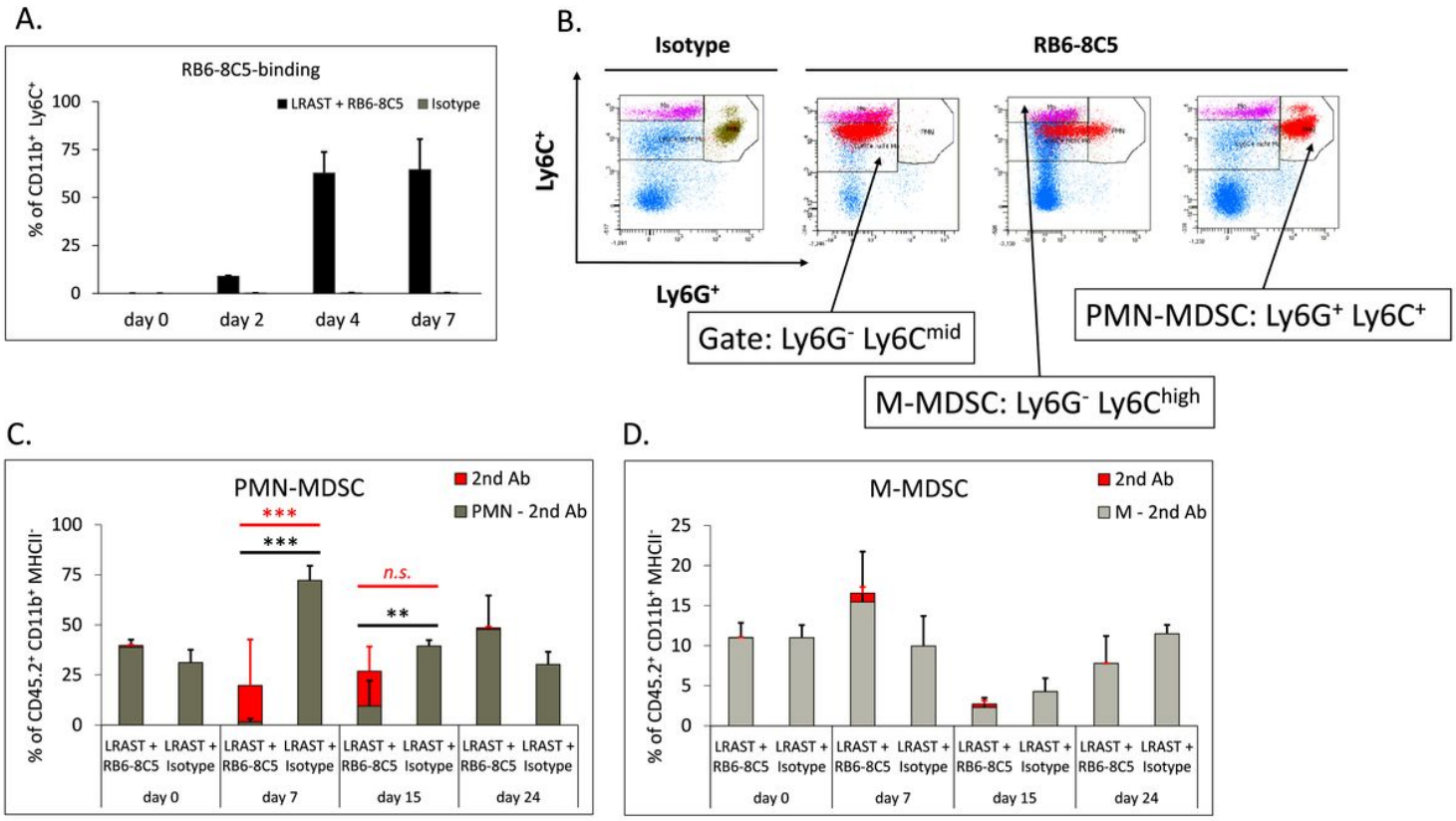

Figure 3

Long-term results of MDSC-depletion and appearance behavior of PMN-MDSC throughout the gates. (A) As assessed by flow cytometry columns represent % of CD11b+ Ly6C+ cells with anti-Gr-1 mAb (RB6-8C5) bound to their cell surface in the blood of mice treated with LRAST + RB6-8C5 compared to mice treated with Isotype Ab alone. RB6-8C5-binding is as indicated by secondary antibody staining. FACS analysis was performed on days 0 (before first RB6-8C5 administration), and days 2, 4, and 7. (B) Representative Ly6G/Ly6C dot-plots with gates for PMN-, M-MDSC, and Ly6Cmid / Ly6G- cells, illustrating appearance of PMN-MDSC when exposed to depleting antibodies (RB6-8C5). Red dots represent RB6-8C5-bound cells, as indicated by secondary antibody staining. (C) Long-term depletion results for PMN-, and M-MDSC, depicted as % of CD45.2+ CD11b+ MHCII- cells on days 0 (before first RB6-8C5 administration), and days 7, 15, and 24 after lymphodepletion. Grey columns represent the amount of PMN- or M-MDSC net of cells with RB6-8C5 surface binding within the same (PMN- or M-MDSC-) gate, respectively. Red columns represent the portion of secondary antibody bound cells (“2nd Ab”) within the PMN- or M-MDSC gate, respectively.

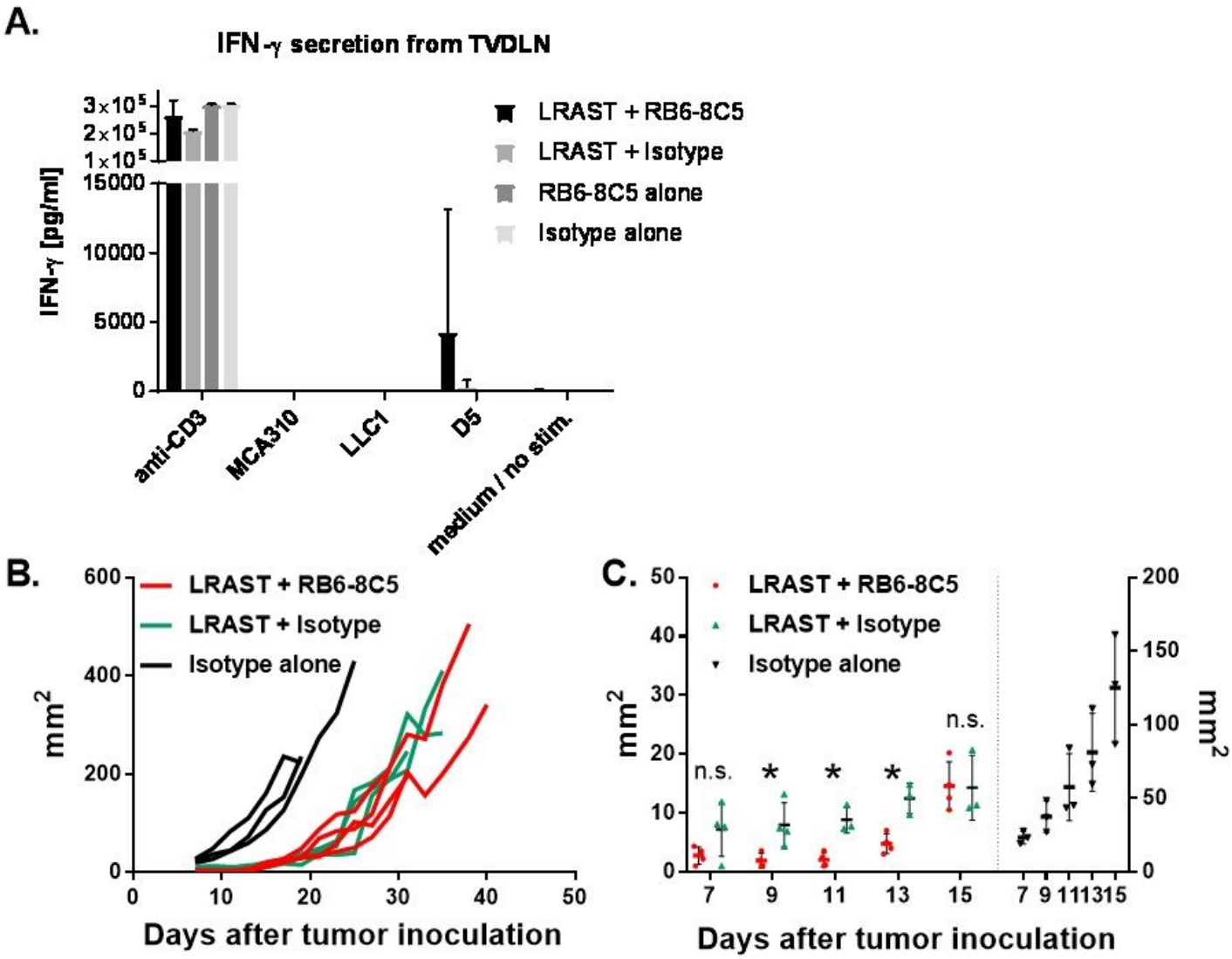

Figure 4

Cytokine response and effect on tumor growth after combining LRAST with anti-Gr-1 antibody treatment. (A) C57BL/6-mice were subcutaneously injected with 20 x 104 D5-cells (5 x 104 at each flank nearby the proximal extremities) and treated according to LRAST w/o MDSC-depletion with anti-Gr-1 mAb (clone RB6-8C5) (n = 2-4 per group). Mice were euthanized on day 9 after lymphodepletion and inguinal as well as axillary lymphatic nodules were harvested. T cells from TVDLN were polyclonally stimulated with anti-CD3 mAb und expanded with IL-2. To assess tumor-specific IFN-γ release, cells were incubated with autologous tumor cells of the D5-lineage or control tumor cell-lines (MCA310 and LLC1). Wells coated with anti-CD3 mAb served as positive controls, and wells with native RPMI cell culture medium represented negative controls. (B) Subcutaneous tumor growth of mice treated with LRAST alone (green), LRAST combined with RB6-8C5 (red), or isotype control (black) (n = 4 for both LRAST groups, n = 3 for isotype control group). Maximum and minimum diameter of the tumors were determined using caliper and the multiplication product (in mm2) depicted against time (in days). Each line represents one mouse

of the respective treatment group. (C) Comparison of mice treated with LRAST alone, versus mice treated with the combination of LRAST and RB6-8C5, focusing on the initial treatment phase (days 7 – 15).

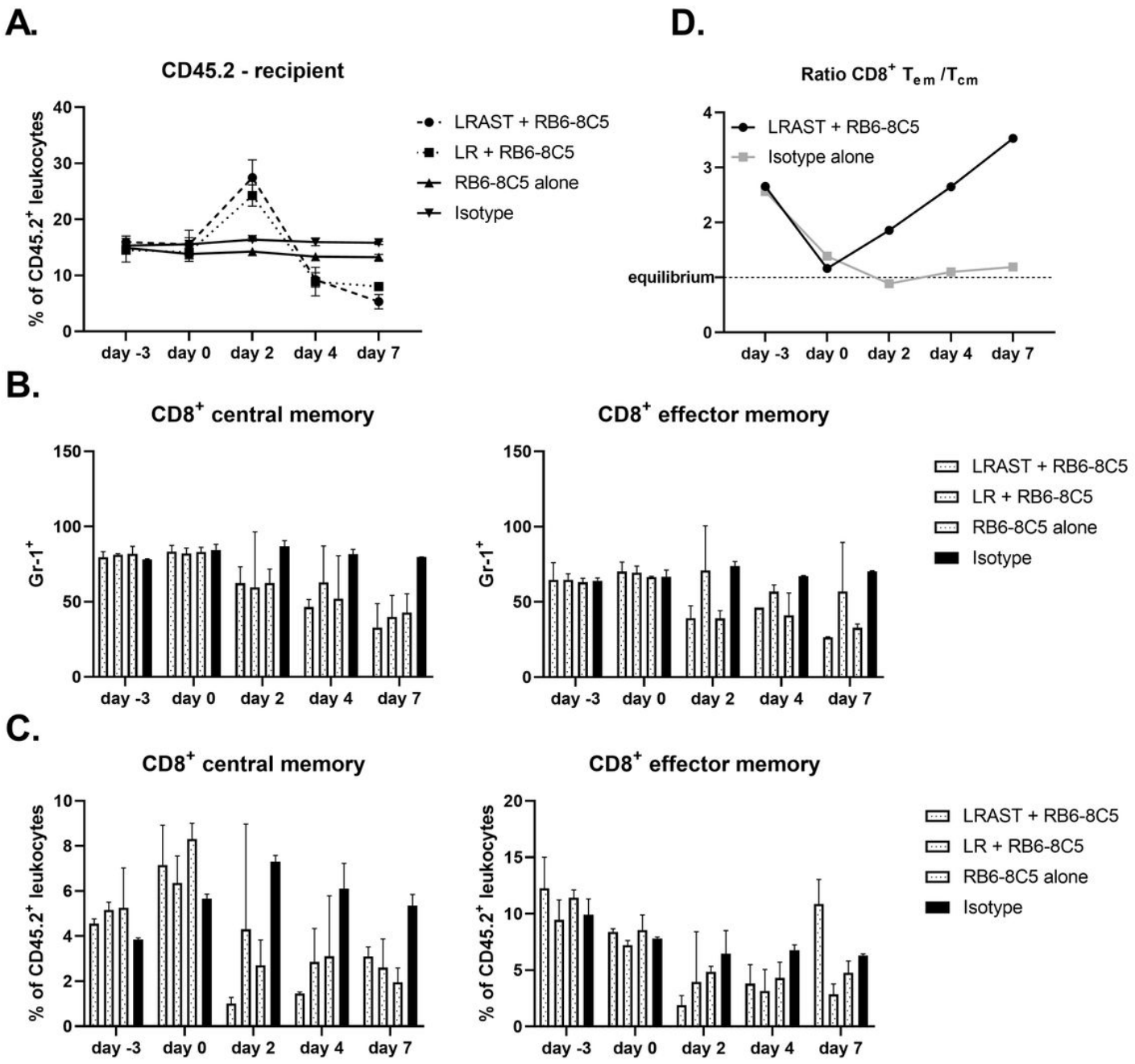

Figure 5

Effect of RB6-8C5 administration on CD8+ memory T cells. (A) Frequency of CD3+ CD8+ cells in % of CD45.2+ leukocytes (in the following referred to as CD8+ cells), assessed by flow cytometry on days -3, 0, 2, 4, and 7 from the blood of mice in different treatment groups (as indicated in the picture). (B) Frequency of Gr-1+ CD8+ central (left) and effector (right) memory T cells from the same animals as in (A). (C) CD8+ central (left) and effector (right) memory T cells in % of CD45.2+ leucocytes form the same animals as in (A). (D) Ratio of CD8+ effector and central memory T cells (Tem/Tcm) calculated from

results depicted in (C). A ratio equal to 1 represents an equilibrium state with identical amounts of both memory T cell subsets.